# Deviations from tribimaximal mixing due to the vacuum expectation value misalignment in $A_4$ models

James Barry* and Werner Rodejohann†

*Max-Planck-Institut für Kernphysik, Postfach 103980, D-69029 Heidelberg, Germany*

(Received 22 March 2010; published 10 May 2010; publisher error corrected )

The addition of an $A_4$ family symmetry and extended Higgs sector to the standard model can generate the tribimaximal mixing pattern for leptons, assuming the correct vacuum expectation value alignment of the Higgs scalars. Deviating this alignment affects the predictions for the neutrino oscillation and neutrino mass observables. An attempt is made to classify the plethora of models in the literature, with respect to the chosen $A_4$ particle assignments. Of these models, two particularly popular examples have been analyzed for deviations from tribimaximal mixing by perturbing the vacuum expectation value alignments. The effect of perturbations on the mixing angle observables is studied. However, it is only investigation of the mass-related observables (the effective mass for neutrinoless double beta decay and the sum of masses from cosmology) that can lead to the exclusion of particular models by constraints from future data, which indicates the importance of neutrino mass in disentangling models. The models have also been tested for fine-tuning of the parameters. Furthermore, a well-known seesaw model is generalized to include additional scalars, which transform as representations of $A_4$ not included in the original model.

DOI: 10.1103/PhysRevD.81.093002 PACS numbers: 14.60.Pq

## I. INTRODUCTION

The experimental evidence of neutrino oscillations implies massive neutrinos, which contradicts the predictions of the standard model (SM). There are currently many experiments focused on precise measurements of the neutrino mass and mixing parameters: neutrino physics can be said to have entered the ''precision era.''

Global fits to the latest neutrino oscillation data [1–4] show that the leptonic mixing, or Pontecorvo-Maki-Nakagawa-Sakata, matrix $U_{\rm PMNS}$ is very close to the tribimaximal mixing (TBM) matrix

$$U_{\rm TBM} \equiv \begin{pmatrix} \frac{2}{\sqrt{6}} & \frac{1}{\sqrt{3}} & 0 \\ -\frac{1}{\sqrt{6}} & \frac{1}{\sqrt{3}} & \frac{1}{\sqrt{2}} \\ -\frac{1}{\sqrt{6}} & \frac{1}{\sqrt{3}} & -\frac{1}{\sqrt{2}} \end{pmatrix}, \qquad (1)$$

first proposed in Ref. [5]. Since the allowed deviations from TBM can only be small (not more than 10–15%), this mixing pattern represents at least a zeroth order approximation to lepton mixing [6]. It is completely different from the mixing in the quark sector, and has motivated extensive research into models of family symmetries [7].

Some of the discrete family symmetries used in the literature are[1]: $A_4$, $S_3$, $S_4$, $T'$, $\Delta(27)$ and $\Sigma(81)$; there are also models that employ continuous symmetries such as $SU(3)$ or $SO(3)$. The $A_4$ models have a very economical structure in terms of group representations and field content. The most general mass matrix leading to TBM can be shown to be invariant under one of the group generators [7] (see the Appendix). Furthermore, the use of $A_4$ can be geometrically motivated: it is the symmetry group of the regular tetrahedron, and the angle between two faces is $2\theta_{\rm TBM}$, where $\sin^2\theta_{\rm TBM} = \frac{1}{3}$. These characteristics have led many authors to construct and/or study models based on $A_4$. Some models generate neutrino masses via effective dimension-5 operators, some apply the type I seesaw mechanism, whereas others use the type II, or the type I + II seesaw mechanisms. Table I is an attempt to classify the vast number of models,[2] according to the chosen $A_4$ assignment of the lepton doublets, lepton singlets and, if appropriate, the seesaw particles.[3] The majority fall into the first four categories.

Very often the TBM scheme is obtained only approximately, or with the cost of fine-tuning and/or various assumptions, such as vacuum expectation value (VEV) alignment. These alignments are chosen, or the models are explicitly constructed, in order to reach alignment, resulting in a certain mixing pattern (in this case TBM). However, corrections to the VEV alignment are expected, be it from renormalization, higher order operators, or the tree-level exchange of heavy fermions, for example. The aim of this paper is to study the effects of VEV-misalignment on the neutrino mass and lepton mixing observables. There already exist some numerical analyses [12,13,31,54,59] focused on specific $A_4$ models. In addition, the effects of higher order operators have been studied in $A_4$ [59] and $S_4$ [64,65] models, where the unperturbed VEV alignments predict exact TBM. This work emphasizes that observables related to neutrino mass (that is, the

*james.barry@mpi-hd.mpg.de
†werner.rodejohann@mpi-hd.mpg.de

[1]See the review in Ref. [7] for a list of references.

[2]An earlier, much less complete classification can be found in [61].

[3]There are also models that use the inverse and linear seesaw mechanisms [62], as well as the inverse type III seesaw mechanism [63], with the same particle assignments as type D models.

 

TABLE I. Particle assignments of $A_4$ models in the literature. Lepton doublets, charged lepton singlets and right-handed neutrinos are denoted by $L_i$, $\ell_i^c$ and $\nu_i^c$, respectively. $\Delta$ denotes the Higgs triplets in the type II seesaw mechanism. Models that also study the quark sector have the superscript #, those that embed $A_4$ into a grand unified theory group have the superscript $*$.

| Type | $L_i$ | $\ell_i^c$ | $\nu_i^c$ | $\Delta$ | References |
|---|---|---|---|---|---|
| A1 | $\underline{3}$ | $\underline{1}$, $\underline{1}'$, $\underline{1}''$ | ... | ... | [8–17][18]# |
| A2 | | | | $\underline{1}$, $\underline{1}'$, $\underline{1}''$, $\underline{3}$ | [19,20] |
| B1 | $\underline{3}$ | $\underline{1}$, $\underline{1}'$, $\underline{1}''$ | $\underline{3}$ | ... | [11,21–24]# [25,26]* [27–38] |
| B2 | | | | $\underline{1}$, $\underline{3}$ | [39]# |
| C1 | $\underline{3}$ | $\underline{3}$ | ... | ... | [9] |
| C2 | | | | $\underline{1}$ | [40,41] [42]# |
| C3 | | | | $\underline{1}$, $\underline{3}$ | [43] |
| C4 | | | | $\underline{1}$, $\underline{1}'$, $\underline{1}''$, $\underline{3}$ | [44] |
| D1 | $\underline{3}$ | $\underline{3}$ | $\underline{3}$ | ... | [45,46]* [47,48] |
| D2 | | | | $\underline{1}$ | [49,50]* |
| D3 | | | | $\underline{1}'$ | [51]* |
| D4 | | | | $\underline{1}'$, $\underline{3}$ | [52]* |
| E | $\underline{3}$ | $\underline{3}$ | $\underline{1}$, $\underline{1}'$, $\underline{1}''$ | ... | [53,54] |
| F | $\underline{1}$, $\underline{1}'$, $\underline{1}''$ | $\underline{3}$ | $\underline{3}$ | $\underline{1}$ or $\underline{1}'$ | [55] |
| G | $\underline{3}$ | $\underline{1}$, $\underline{1}'$, $\underline{1}''$ | $\underline{1}$, $\underline{1}'$, $\underline{1}''$ | ... | [56] |
| H | $\underline{3}$ | $\underline{1}$, $\underline{1}$, $\underline{1}$ | ... | ... | [57] |
| I | $\underline{3}$ | $\underline{1}$, $\underline{1}$, $\underline{1}$ | $\underline{1}$, $\underline{1}$, $\underline{1}$ | ... | [58]* |
| J | $\underline{3}$ | $\underline{1}$, $\underline{1}$, $\underline{1}$ | $\underline{3}$ | ... | [59,60] |

TABLE II. Best-fit values and allowed $n\sigma$ ranges for the global three flavor neutrino oscillation parameters, from Ref. [3].

| Parameter | $\Delta m^2_{21}(10^{-5}\ \mathrm{eV}^2)$ | $\sin^2\theta_{12}$ | $\sin^2\theta_{13}$ | $\sin^2\theta_{23}$ | $\lvert\Delta m^2_{31}\rvert(10^{-3}\ \mathrm{eV}^2)$ |
|---|---|---|---|---|---|
| Best-fit | 7.67 | 0.312 | 0.016 | 0.466 | 2.39 |
| $1\sigma$ range | 7.48–7.83 | 0.294–0.331 | 0.006–0.026 | 0.408–0.539 | 2.31–2.50 |
| $2\sigma$ range | 7.31–8.01 | 0.278–0.352 | $<0.036$ | 0.366–0.602 | 2.19–2.66 |
| $3\sigma$ range | 7.14–8.19 | 0.263–0.375 | $<0.046$ | 0.331–0.644 | 2.06–2.81 |

effective mass for neutrinoless double beta decay ($0\nu\beta\beta$) and the sum of neutrino masses for cosmology) provide the best possibility to disentangle the models. Furthermore, and in contrast to previous studies, a more general VEV-misalignment is allowed for. The analysis in the present paper is focused on models of types A and B that predict TBM, as well as generalizations of these models to include more Higgs singlets.

In this analysis,[4] the chosen VEV alignment is modified by random complex deviations, perturbing the neutrino and charged lepton mass matrices from their original structure ($M_\nu$ and $M_\ell$) to the perturbed ones, $M'_\nu$ and $M'_\ell$. The resulting neutrino mixing angles and mass-squared differences can be compared with current data (Table II). The well-known standard parametrization of the PMNS mixing matrix is

$$U_{\mathrm{PMNS}} = \begin{pmatrix} c_{12}c_{13} & s_{12}c_{13} & s_{13}e^{-i\delta} \\ -s_{12}c_{23} - c_{12}s_{23}s_{13}e^{i\delta} & c_{12}c_{23} - s_{12}s_{23}s_{13}e^{i\delta} & s_{23}c_{13} \\ s_{12}s_{23} - c_{12}c_{23}s_{13}e^{i\delta} & -c_{12}s_{23} - s_{12}c_{23}s_{13}e^{i\delta} & c_{23}c_{13} \end{pmatrix} \begin{pmatrix} 1 & 0 & 0 \\ 0 & e^{i\lambda_2} & 0 \\ 0 & 0 & e^{i\lambda_3} \end{pmatrix}, \tag{2}$$

where $c_{ij} \equiv \cos\theta_{ij}$, $s_{ij} \equiv \sin\theta_{ij}$ and $\theta_{12}$, $\theta_{13}$, $\theta_{23}$ ($0 \leq \theta_{ij} \leq \pi/2$) are the three mixing angles. There are three phases in Eq. (2): $\delta$ is the $CP$ violating Dirac phase, and $\lambda_2$ and $\lambda_3$ are Majorana phases, with $0 \leq \delta, \lambda_2, \lambda_3 \leq 2\pi$. The two Majorana phases, $\lambda_2$ and $\lambda_3$, do not affect the neutrino oscillation probability, but have an influence on the amplitude for $0\nu\beta\beta$.

One can also perform a "fine-tuning test" for each model, by examining the values that the mass matrix parameters must take in order to give the correct mass-squared differences, before perturbations are applied. Since these parameters generally originate from the prod-

[4]Other approaches to deviations from TBM can be found in Refs. [66–73].

uct of some coupling constant with the VEV of a Higgs scalar, any close relationship between the parameters is highly unlikely, and could be evidence of fine-tuning in a particular model [13].

The paper is built up as follows: in Sec. II a type A model is introduced, it is examined for fine-tuning, the addition of Higgs singlets is discussed, and the model is analyzed for deviations from TBM; in Sec. III the same procedure is followed for a type B seesaw model. Section IV presents the summary and conclusions, and for the sake of completeness there is a discussion of the $A_4$ group in the Appendix.

## II. THE ORIGINAL MA/ALTARELLI-FERUGLIO TYPE A MODEL

In type A models, lepton doublets transform as $\underline{3}$, charged lepton singlets as $\underline{1}$, $\underline{1}'$, $\underline{1}''$, and right-handed neutrinos are absent. In this case the neutrino mass usually comes from dimension-5 operators. Although Table I contains a long list of references for type A models, many of these works are phenomenological analyses of the same few models. The original model by Ma [19] is further developed in Ref. [8], where also an extra-dimensional solution to the vacuum alignment problem is provided.[5]

The models in Refs. [8,19] employ the so-called Ma-Rajasekaran (M-R) basis for $A_4$, in which neither $M_\nu$ nor $M_\ell$ is diagonal, but the product of the mixing matrices in each sector leads to TBM. In order to connect $A_4$ models with the modular symmetry and thus the larger framework of string theory, the same model can be formulated [11] in a different basis for $A_4$ [the Altarelli-Feruglio (A-F) basis]. In this basis the charged leptons immediately come out as diagonal, which means that the neutrino mass matrix is in the flavor basis, and is diagonalized by the TBM matrix. The two bases are simply related by a unitary transformation, and the multiplication rules differ (see the Appendix for details).

### A. The original model in the A-F basis

Along with the usual type A particle assignments for leptons (Table I), this model has two SM Higgs doublets, which are invariant under $A_4$, as well as two $A_4$ triplets $\varphi$ and $\varphi'$, and an $A_4$ singlet $\xi$, all three of which are gauge singlets (Table III). These particle assignments, along with the $A_4$ multiplication rules, lead to the Lagrangian

$$\begin{aligned}\mathcal{L}_Y = {} & y_e e^c(\varphi L) + y_\mu \mu^c(\varphi L)' + y_\tau \tau^c(\varphi L)'' \\ & + x_a \xi(LL) + x_d(\varphi' LL) \\ & [+x_c \xi'(LL)'' + x_b \xi''(LL)'] + \text{H.c.} + \ldots, \end{aligned} \quad (3)$$

where $(\underline{3}\,\underline{3})$ transforms as $\underline{1}$, $(\underline{3}\,\underline{3})'$ transforms as $\underline{1}'$, and $(\underline{3}\,\underline{3})''$ transforms as $\underline{1}''$, and $y_\alpha$, $x_a$ and $x_d$ are dimensionless coupling constants. The notation in Eq. (3) follows the simplified description from Ref. [11], where the Higgs doublet fields $h_u$ and $h_d$, and the cutoff scale $\Lambda$ are set to 1. Thus the term $y_e e^c(\varphi L)$ is in fact $y_e e^c(\varphi L) h_d/\Lambda$, $x_a \xi(LL)$ is short for $x_a \xi(L h_u L h_u)/\Lambda^2$ and so on. The dots stand for higher dimensional operators—in this model these are suppressed by additional powers of the cutoff $\Lambda$, as long as the VEVs are sufficiently smaller than $\Lambda$. The two terms in parenthesis on the third line of Eq. (3) come from additional Higgs singlets; these were not part of the original model, but one can show [13] that TBM can still be achieved with either two or three Higgs singlets in this model. This will be discussed in Secs. II B and II C.

TABLE III. Particle assignments of the A-F $A_4$ model. There is also an additional $Z_3$ symmetry, which decouples the charged lepton and neutrino sectors, and a $U(1)$ symmetry to generate the hierarchy of charged lepton masses.

| Lepton | $SU(2)_L$ | $A_4$ |
|---|---|---|
| $L$ | 2 | $\underline{3}$ |
| $e^c$ | 1 | $\underline{1}$ |
| $\mu^c$ | 1 | $\underline{1}''$ |
| $\tau^c$ | 1 | $\underline{1}'$ |
| Scalar | | |
| $h_u$ | 2 | $\underline{1}$ |
| $h_d$ | 2 | $\underline{1}$ |
| $\varphi$ | 1 | $\underline{3}$ |
| $\varphi'$ | 1 | $\underline{3}$ |
| $\xi$ | 1 | $\underline{1}$ |

Upon symmetry breaking, the VEVs of the Higgs singlet and triplets take the alignments

$$\langle \xi \rangle = u_a, \qquad \langle \varphi \rangle = (v, 0, 0) \quad \text{and} \quad \langle \varphi' \rangle = (v', v', v'), \quad (4)$$

which lead to the charged lepton mass matrix

$$M_\ell = v_d \frac{v}{\Lambda} \begin{pmatrix} y_e & 0 & 0 \\ 0 & y_\mu & 0 \\ 0 & 0 & y_\tau \end{pmatrix}, \quad (5)$$

where $v_d$ is the VEV of the Higgs doublet $h_d$. Thus the charged fermion masses are

$$m_e = y_e v_d \frac{v}{\Lambda}, \qquad m_\mu = y_\mu v_d \frac{v}{\Lambda}, \qquad m_\tau = y_\tau v_d \frac{v}{\Lambda}. \quad (6)$$

When only one Higgs singlet ($\xi \sim \underline{1}$) is present, the neutrino mass matrix is

$$M_\nu^{(1)} = m_0 \begin{pmatrix} a + \frac{2d}{3} & -\frac{d}{3} & -\frac{d}{3} \\ \cdot & \frac{2d}{3} & a - \frac{d}{3} \\ \cdot & \cdot & \frac{2d}{3} \end{pmatrix}, \quad (7)$$

with $m_0 = \frac{v_u^2}{\Lambda}$, $a = 2x_a \frac{u_a}{\Lambda}$ and $d = 2x_d \frac{v'}{\Lambda}$, where $v_u$ is the

[5]Note that the model in Ref. [19] contains 6 Higgs triplets, whereas the model in Ref. [8] uses dimension-5 operators.

VEV of $h_u$. The neutrino mass matrix is diagonalized by the transformation

$$U^T M_\nu U = \frac{v_u^2}{\Lambda}\,\mathrm{diag}(a+d, a, -a+d), \tag{8}$$

with $U = U_{\rm TBM}$, as in Eq. (1). Thus TBM is achieved, and the neutrino masses are $m_1 = m_0(a+d)$, $m_2 = m_0 a$ and $m_3 = m_0(-a+d)$, which results in the sum-rule $2m_2 + m_3 = m_1$. Here the masses are understood to be complex, with the Majorana phases still attached. Note that with only one Higgs singlet it is impossible to get the inverted mass hierarchy in this model, as shown in Ref. [13].

It is interesting to note that in the case of one Higgs singlet, with the mass matrix in Eq. (7), some fine-tuning is required between the parameters $a$ and $d$ for the model to give the correct neutrino mass-squared differences [13]. This seems rather contrived, since $a$ and $d$ come from the products of different Yukawa couplings with the VEVs of the Higgs singlet $\xi$ and triplet $\varphi'$, respectively. As can be seen in Fig. 1, if both $a$ and $d$ are real (as in Ref. [13]), there is a linear relationship between the two parameters. If $d$ is complex (as in this analysis), there is only a slightly greater allowed region in the $a-d$ parameter space. Note that w.l.o.g., $a$ can be chosen to be real. There are no perturbations applied in this case, and the parameter $m_0$ is set to 0.025 eV, the typical scale for the mass matrix of normally ordered neutrinos. In later cases, where the inverted mass ordering is studied, $m_0$ is fixed to 0.05 eV. The magnitudes of the parameters $a$ and $d$ (and later also $c$) are randomly varied in the range $|a, c, d| \leq 4$, with their complex phases varying from zero to $2\pi$.

### B. Two Higgs singlets

Recall that only one Higgs singlet is introduced in the original model (Table III). However, in the framework of $A_4$ symmetry it is natural to take advantage of all representations of the group, and in this model it is also possible to achieve TBM with both two and/or three Higgs singlets [13]. In addition to the Higgs singlet $\xi$, the singlets $\xi'$ and $\xi''$ can be introduced [Eq. (4)], transforming as $\underline{1}'$ and $\underline{1}''$ under $A_4$, respectively. The new singlets have the VEVs

$$\langle \xi' \rangle = u_c \quad \text{and} \quad \langle \xi'' \rangle = u_b. \tag{9}$$

With only two Higgs singlets, there are three possible combinations ($\xi$, $\xi'$; $\xi$, $\xi''$ and $\xi'$, $\xi''$), but one can show [13] that only the singlets $\xi'$ and $\xi''$ can give rise to TBM. In this case, the resulting mass matrix is

$$M_\nu^{(2)} = m_0 \begin{pmatrix} \frac{2d}{3} & b - \frac{d}{3} & c - \frac{d}{3} \\ \cdot & c + \frac{2d}{3} & -\frac{d}{3} \\ \cdot & \cdot & b + \frac{2d}{3} \end{pmatrix}, \tag{10}$$

where $b = 2x_b \frac{u_b}{\Lambda}$ and $c = 2x_c \frac{u_c}{\Lambda}$. An additional condition for TBM is that $b = c$, which is a consequence of the necessary $\mu - \tau$ symmetry,[6] and with this constraint the eigenvalues turn out to be $m_1 = m_0(-c+d)$, $m_2 = 2m_0 c$ and $m_3 = m_0(c+d)$, with the new sum-rule $m_3 - m_1 = m_2$. In this case, w.l.o.g., $c$ can be chosen to be real. The scatter plots in Fig. 2 show that the $c-d$ parameter space is quite tightly constrained (note that with additional Higgs singlets, the inverted mass hierarchy is now possible).

### C. Three Higgs singlets

If all three singlets ($\xi$, $\xi'$ and $\xi''$) are present, the resulting mass matrix is

$$M_\nu^{(3)} = m_0 \begin{pmatrix} a + \frac{2d}{3} & b - \frac{d}{3} & c - \frac{d}{3} \\ \cdot & c + \frac{2d}{3} & a - \frac{d}{3} \\ \cdot & \cdot & b + \frac{2d}{3} \end{pmatrix}, \tag{11}$$

and the requirement for exact TBM is that $a \neq b = c$, which again reflects the necessary $\mu - \tau$ symmetry.[7] Here one can choose real $a$ and complex $c$ and $d$, w.l.o.g. This case is equivalent to the original Ma model in Ref. [19], and here there is more freedom in choosing parameters, as can be seen from the scatter plots of $a - c - d$ parameter space in Fig. 3. There is basically no more tuning necessary in order to generate the correct mass-squared differences. The eigenvalues of the mass matrix in Eq. (11), with $a \neq b = c$, are $m_1 = m_0(a - c + d)$, $m_2 = m_0(a + 2c)$ and $m_3 = m_0(-a + c + d)$.

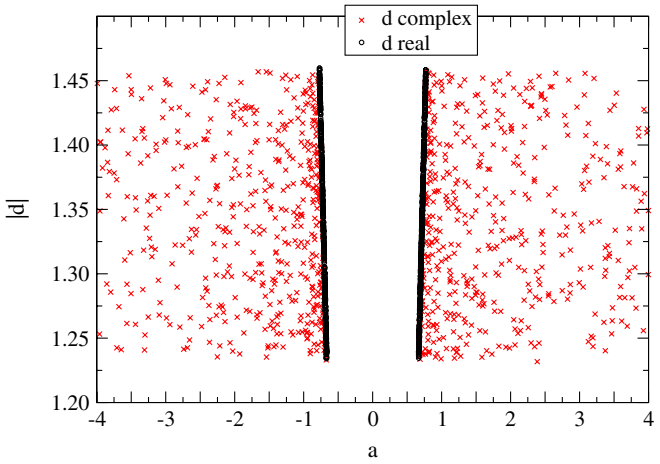


FIG. 1 (color online). Scatter plot showing allowed regions (for the $3\sigma$ ranges of the oscillation parameters) in the $a-d$ parameter space for the original A-F model, with one Higgs singlet, normal hierarchy and TBM.

[6] Although $\mu - \tau$ symmetry is required to get TBM, this forces one to impose the *ad hoc* relation $b = c$.

[7] It can be shown [13] that the conditions $a = b = c$, $a = b \neq c$ and $a = c \neq b$ do not simultaneously give TBM and the correct mass spectrum.

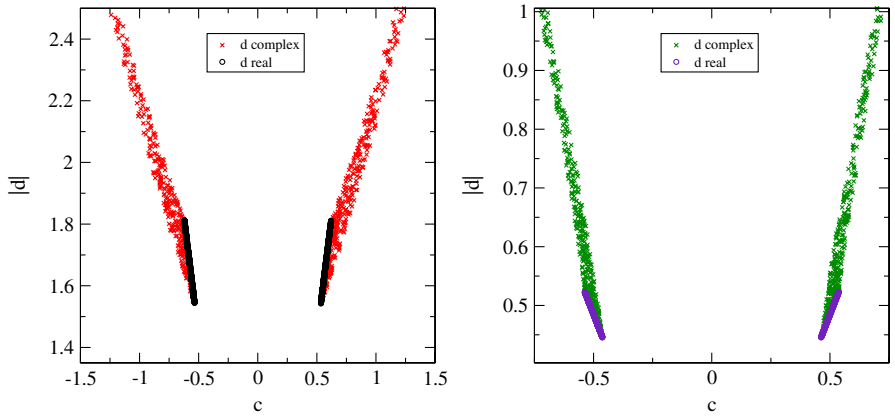


(a) Normal hierarchy (b) Inverted hierarchy

FIG. 2 (color online). Scatter plots of the $c - d$ parameter space for the A-F model with two Higgs singlets [Eq. (11)], for normal and inverted hierarchy, with the condition $b = c$. In order to emphasize the difference between the complex and real case, the entire parameter space is not shown: in the complex case $|d|$ ranges up to 4 for the normal hierarchy and 2.5 for the inverted hierarchy.

### D. Deviations from TBM in the A-F model

The three mass matrices in Eqs. (7), (10), and (11) are phenomenologically interesting, and will be numerically analyzed below. In order to study deviations from TBM, the VEV alignments of the Higgs triplets are perturbed, so that

$$\begin{aligned} \langle \varphi \rangle &= (v, v\epsilon_1^{\mathrm{ch}}, v\epsilon_2^{\mathrm{ch}}) \quad \text{and} \\ \langle \varphi' \rangle &= (v', v'(1+\epsilon_1), v'(1+\epsilon_2)). \end{aligned} \tag{12}$$

Furthermore, in the cases of two and three Higgs singlets,

$$b = c(1+\epsilon_3) \tag{13}$$

is defined in order to study the effect of changing the relative alignment of the Higgs singlets. Recall that the condition $b = c$ is necessary for TBM in both the two and three singlet cases.

With the above VEV-misalignment, the charged lepton mass matrix becomes

$$M_\ell' = v_d \frac{v}{\Lambda} \begin{pmatrix} y_e & y_e\epsilon_2^{\mathrm{ch}} & y_e\epsilon_1^{\mathrm{ch}} \\ y_\mu\epsilon_1^{\mathrm{ch}} & y_\mu & y_\mu\epsilon_2^{\mathrm{ch}} \\ y_\tau\epsilon_2^{\mathrm{ch}} & y_\tau\epsilon_1^{\mathrm{ch}} & y_\tau \end{pmatrix}. \tag{14}$$

In the unperturbed case, the mass of each charged lepton $l_\alpha$ is $m_\alpha = y_\alpha v_d \frac{v}{\Lambda}$ [Eq. (6)]. In this analysis, the mass scale $v_d \frac{v}{\Lambda}$ is fixed to the tau mass, and each of the coefficients $y_e$, $y_\mu$ and $y_\tau$ are varied randomly by 10% around their unperturbed values. Note that the charged lepton sector is unaffected by additional Higgs singlets, due to the presence of a $Z_3$ symmetry (Table III).

The deviated neutrino mass matrix with one Higgs singlet is

$$M_\nu^{(1)\prime} = m_0 \begin{pmatrix} a + \frac{2d}{3} & -\frac{d}{3}(1+\epsilon_2) & -\frac{d}{3}(1+\epsilon_1) \\ \cdot & \frac{2d}{3}(1+\epsilon_1) & a - \frac{d}{3} \\ \cdot & \cdot & \frac{2d}{3}(1+\epsilon_2) \end{pmatrix}, \tag{15}$$

and with two Higgs singlets ($\xi'$ and $\xi''$) is

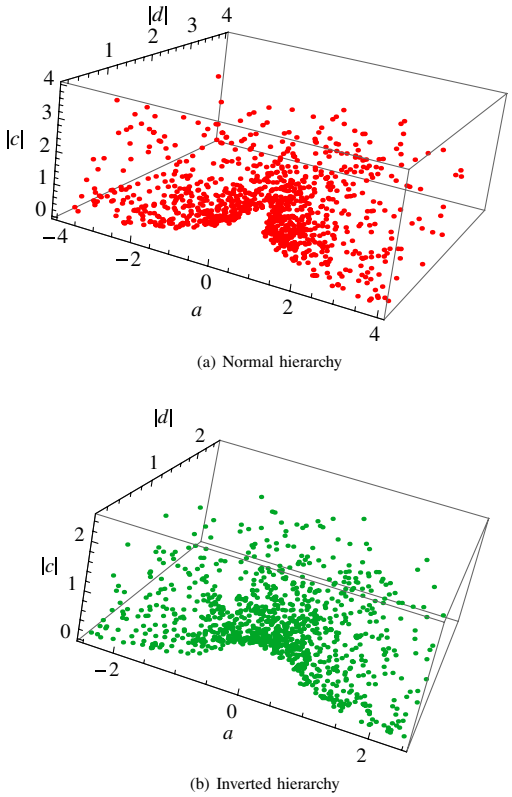


(a) Normal hierarchy

(b) Inverted hierarchy

FIG. 3 (color online). Scatter plots of the $a - c - d$ parameter spaces for the A-F model with three Higgs singlets [Eq. (11)], for normal and inverted hierarchy, with the condition $b = c$.

$$M_\nu^{(2)\prime} = m_0 \begin{pmatrix} \frac{2d}{3} & c(1+\epsilon_3) - \frac{d}{3}(1+\epsilon_2) & c - \frac{d}{3}(1+\epsilon_1) \\ \cdot & c + \frac{2d}{3}(1+\epsilon_1) & -\frac{d}{3} \\ \cdot & \cdot & c(1+\epsilon_3) + \frac{2d}{3}(1+\epsilon_2) \end{pmatrix}. \tag{16}$$

The most general case (three Higgs singlets) is

$$M_\nu^{(3)\prime} = m_0 \begin{pmatrix} a + \frac{2d}{3} & c(1+\epsilon_3) - \frac{d}{3}(1+\epsilon_2) & c - \frac{d}{3}(1+\epsilon_1) \\ \cdot & c + \frac{2d}{3}(1+\epsilon_1) & a - \frac{d}{3} \\ \cdot & \cdot & c(1+\epsilon_3) + \frac{2d}{3}(1+\epsilon_2) \end{pmatrix}, \tag{17}$$

where the condition $a \neq c$ still holds. One proceeds by diagonalizing the matrices in Eqs. (15)–(17). The perturbation parameters are in general complex, and the range $|\epsilon_i^{(\mathrm{ch})}| \leq 0.3$ is used throughout this work, with the phases varied freely. W.l.o.g., one can choose the parameters $\epsilon_1$ and $\epsilon_1^{\mathrm{ch}}$ to be real. The other parameters $a$, $b$ and $d$ are varied as before, and $m_0$ is also fixed as described above.

It is interesting to compare the deviations from TBM for different numbers of Higgs singlets, with the same perturbations applied to $M_\ell$ in each case [Eq. (14)]. Figure 4 shows the results for the normal mass hierarchy (it is impossible to get the inverted hierarchy with one Higgs singlet). There are small differences, and in general one can conclude that with more singlets, greater deviation from TBM is possible. However, it is evident that if VEV alignment deviations are applied, the $A_4$ models deviate from TBM in a rather random fashion, and it is difficult to draw any firm conclusions from the plots of mixing angle observables.

In contrast, the mass-dependent observables $\sum m_i$ (the sum of absolute neutrino masses) and $\langle m_{ee} \rangle$ (the effective mass for $0\nu\beta\beta$) allow for comparison between the three cases presented above (Fig. 5), and can in principle be used to rule out some cases. These two observables are explicitly given as

$$\sum m_i = m_1 + m_2 + m_3 \quad \text{and} \qquad \langle m_{ee} \rangle = |U_{e1}^2 m_1 + U_{e2}^2 m_2 + U_{e3}^2 m_3|. \tag{18}$$

It is useful to plot these two quantities against each other, in both the unperturbed and perturbed case. The solid black lines in Fig. 5 represent the allowed ranges for normal and inverted ordering, using the best-fit values of the oscillation parameters from Table II, and varying the Majorana phases. The dotted and dashed lines include the $3\sigma$ variation in the oscillation data, for normal and inverted ordering, respectively. The scatter plots display the results of the analysis discussed above. The deviations from TBM lead to more overlap between the normal and inverted hierarchies, with two and three Higgs singlets. Increasing the number of Higgs singlets effectively increases the allowed range for both $\langle m_{ee} \rangle$ and $\sum m_i$. To give one example of the consequences of Fig. 5, note from the middle left panel that if $\langle m_{ee} \rangle$ is experimentally determined to be less than about 0.02 eV, the case with two singlets and normal mass hierarchy can be ruled out.

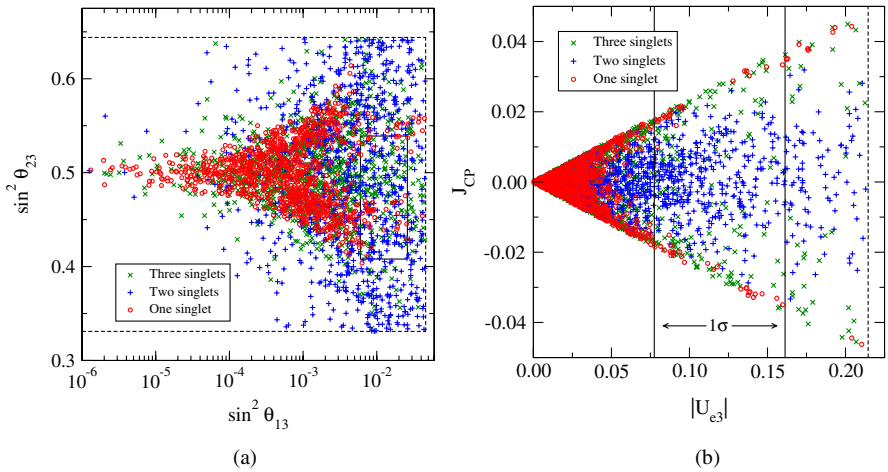


FIG. 4 (color online). Scatter plots of (a) $\sin^2\theta_{23}$ against $\sin^2\theta_{13}$ and (b) $J_{CP}$ against $|U_{e3}|$ for the A-F model, normal hierarchy, with one (red circles), two (blue plus signs) and three (green crosses) Higgs singlets. The solid and dashed lines denote the $1\sigma$ and $3\sigma$ allowed regions, respectively.

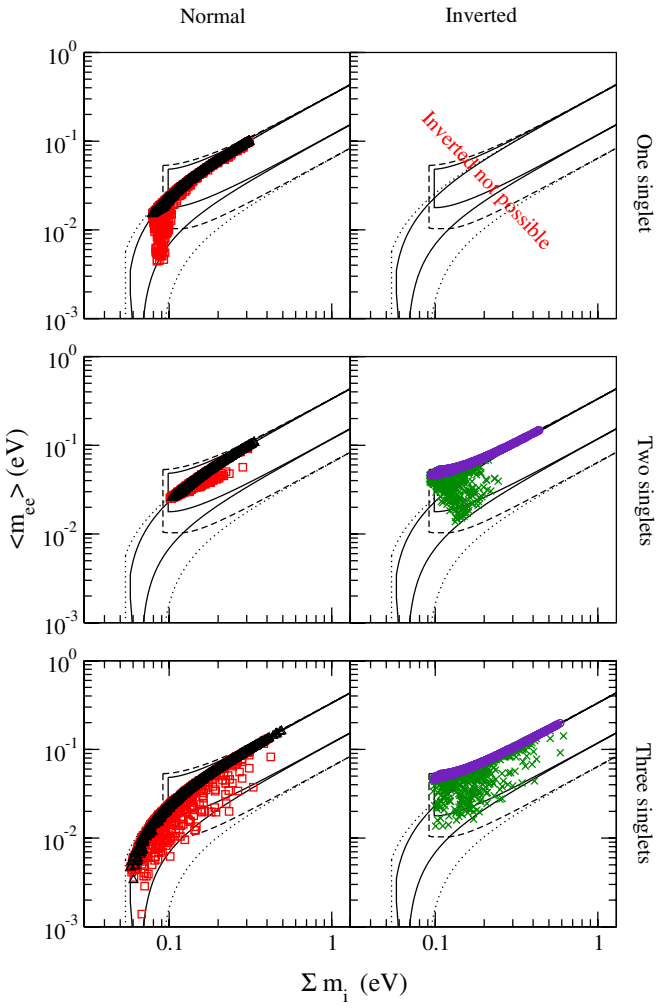


FIG. 5 (color online). Scatter plots of $\langle m_{ee}\rangle$ against $\sum m_i$ for the original A-F model, with one, two and three Higgs singlets. Black triangles (red squares) denote the normal hierarchy unperturbed (perturbed) case; indigo circles (green crosses) denote the inverted hierarchy unperturbed (perturbed) case.

In general, i.e., without any model constraining the mass matrices, it is possible for $\langle m_{ee}\rangle$ to vanish for the normal mass hierarchy. In the case of one Higgs singlet, for example, vanishing $\langle m_{ee}\rangle$ means that the (1,1) entry of the mass matrix in Eq. (7) (or Eq. (15) in the perturbed case) is zero, i.e., $a = 2d/3$. Using the mass eigenvalues from Eq. (8), it follows that the ratio of mass-squared differences is

$$r = \frac{\Delta m^2_{21}}{\Delta m^2_{31}} = \frac{2a+d}{4a} = \frac{1}{8}, \tag{19}$$

which is inconsistent with the data ($r$ should be close to $1/30$). Perturbing the VEV alignment [Eq. (15)] and setting the (1,1) entry of $M_\nu^{(1)\prime}$ to zero gives $r \simeq \frac{1}{8}(1+\epsilon_2-3\epsilon_1)$, which can become sufficiently small. Indeed, in the plot $\langle m_{ee}\rangle$ can take values well below $10^{-2}$ eV. Similar evaluations can be made for the other cases, in this and the next section.

## III. THE ALTARELLI-FERUGLIO TYPE B SEESAW MODEL

According to the classification introduced in Table I, type B models have lepton doublets transforming as $\underline{3}$, charged lepton singlets as $\underline{1}$, $\underline{1}'$, $\underline{1}''$, and right-handed neutrinos transforming as $\underline{3}$. Neutrino mass can be generated by the type I seesaw mechanism or, when weak scalar triplets are introduced, with the type I + II seesaw mechanism.

### A. The original A-F seesaw model

The model in Sec. II A can be extended by introducing right-handed neutrino fields $\nu^c$, transforming as $\underline{3}$ under $A_4$ [11]. The new Lagrangian contains all the terms in Eq. (3), along with the additional terms

$$\begin{aligned}\mathcal{L}_{\mathrm{Y(seesaw)}} = {} & y(\nu^c L)h_u + x_A\xi(\nu^c\nu^c) + x_D(\varphi'\nu^c\nu^c) \\ & [+x_C\xi'(\nu^c\nu^c)'' + x_B\xi''(\nu^c\nu^c)'] \\ & + \mathrm{H.c.} + \ldots,\end{aligned} \tag{20}$$

where $y$ is a coupling constant.[8] Most details of the model, including the VEV alignment in Eq. (4), remain the same, with the charged lepton mass matrix given by Eq. (5). The Dirac mass matrix $M_\nu^D$ is $y v_u$ times the identity matrix, and the Majorana mass matrix is

$$M_R = \begin{pmatrix} a+\frac{2d}{3} & -\frac{d}{3} & -\frac{d}{3} \\ \cdot & \frac{2d}{3} & a-\frac{d}{3} \\ \cdot & \cdot & \frac{2d}{3} \end{pmatrix}\Lambda, \tag{21}$$

where $a = 2x_A\frac{u_a}{\Lambda}$ and $d = 2x_D\frac{v'}{\Lambda}$. With the type I seesaw mechanism ($M_\nu = (M_\nu^D)^T M_R^{-1} M_\nu^D$), the light neutrino mass matrix is

$$M_\nu^{(1)} = \frac{m_0}{3a(a+d)}\begin{pmatrix} 3a+d & d & d \\ \cdot & \frac{2ad+d^2}{d-a} & \frac{d^2-ad-3a^2}{d-a} \\ \cdot & \cdot & \frac{2ad+d^2}{d-a} \end{pmatrix}, \tag{22}$$

with $m_0 = y^2\frac{v_u^2}{\Lambda}$. As in Eq. (8), the matrix in Eq. (22) is diagonalized by the TBM matrix, with eigenvalues $m_1 = m_0/(a+d)$, $m_2 = m_0/a$ and $m_3 = m_0/(-a+d)$, leading to the sum-rule $2/m_2 + 1/m_3 = 1/m_1$. Note that the inverted hierarchy is possible in the seesaw version of this model, even with only one Higgs singlet.

The fine-tuning test again shows that in order for the correct values of the mass-squared differences to be reproduced, the parameters $a$ and $d$ must take rather specific values, as shown in Fig. 6. There is a similar amount of tuning as in the A-F model without seesaw (see Fig. 1).

[8] In Eq. (20) the compact notation of Eq. (3) does not apply.

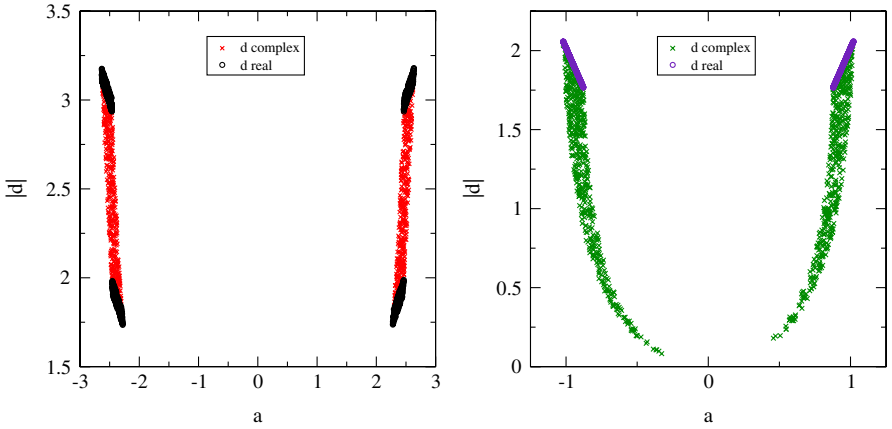


(a) Normal hierarchy (b) Inverted hierarchy

FIG. 6 (color online). Scatter plots of the $a - d$ parameter space for the A-F seesaw model, with one Higgs singlet, for normal and inverted hierarchy.

### B. Two Higgs singlets in the seesaw model

In the original A-F model, the addition of extra Higgs singlets still allows for TBM, with certain conditions (Secs. II B and II C). This idea can also be applied to the seesaw version of the model. Again, it is possible to introduce singlets $\xi'$ and $\xi''$, transforming as $\underline{1}'$ and $\underline{1}''$, respectively. However, just like the nonseesaw case, the singlet combinations $\xi$, $\xi'$ and $\xi$, $\xi''$ cannot give rise to TBM. That is only achieved with the two singlets $\xi'$ and $\xi''$, resulting in the light neutrino mass matrix

$$M_\nu^{(2)} = \frac{m_0}{m^{(2)}} \begin{pmatrix} -d^2 - 2(b+c)d - 3bc & 3b^2 + db + (c-d)d & 3c^2 + dc + (b-d)d \\ \cdot & 3c^2 - d^2 - 2(b+c)d & (c-d)d + b(d-3c) \\ \cdot & \cdot & 3b^2 - d^2 - 2(b+c)d \end{pmatrix}, \tag{23}$$

with $m^{(2)} = 3(b^3 + c^3 - (b+c)d^2)$, $b = 2x_B \frac{u_b}{\Lambda}$ and $c = 2x_C \frac{u_c}{\Lambda}$. The condition $b = c$ is required for exact TBM, as before, and once again the $Z_3$ symmetry means that the charged lepton sector is unaffected. The neutrino mass eigenvalues are $m_1 = m_0/(-c+d)$, $m_2 = m_0/2c$ and $m_3 = m_0/(c+d)$, and the mass sum-rule $1/m_3 - 1/m_1 = 1/m_2$ applies. The scatter plots in Fig. 7 show the allowed regions in $c - d$ parameter space, and exhibit a similar level of tuning as the one singlet case (Fig. 6).

### C. Three Higgs singlets in the seesaw model

If there are three Higgs singlets present, the light neutrino mass matrix is given by

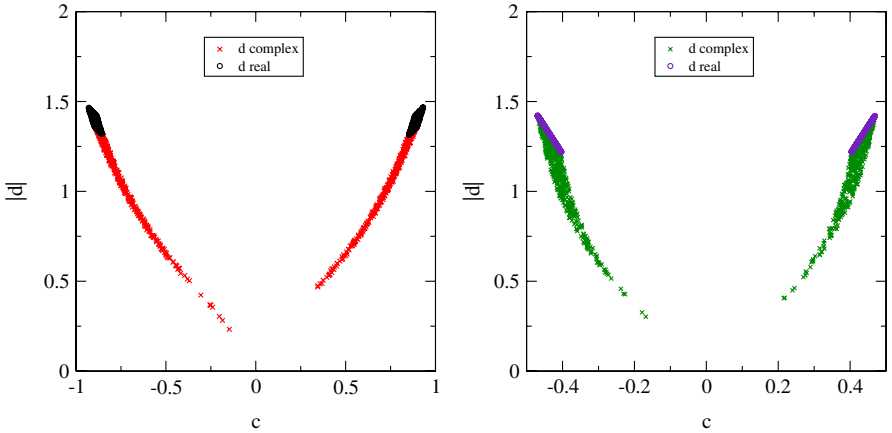


(a) Normal hierarchy (b) Inverted hierarchy

FIG. 7 (color online). Scatter plots of the $c - d$ parameter space for the A-F seesaw model, with two Higgs singlet, for normal and inverted hierarchy.

$$M_\nu^{(3)} = \frac{m_0}{m^{(3)}} M^{(3)}, \tag{24}$$

where the elements of the symmetric matrix $M^{(3)}$ are

$$M_{11}^{(3)} = 3a^2 - d^2 - 3bc - 2(a+b+c)d, \tag{25}$$

$$M_{12}^{(3)} = -d^2 + (a+b+c)d + 3(b^2 - ac), \tag{26}$$

$$M_{13}^{(3)} = 3c^2 + (b+c-d)d + a(d-3b), \tag{27}$$

$$M_{22}^{(3)} = 3c^2 - d^2 - 3ab - 2(a+b+c)d, \tag{28}$$

$$M_{23}^{(3)} = 3a^2 + da - 3bc + (b+c-d)d, \tag{29}$$

$$M_{33}^{(3)} = 3b^2 - d^2 - 3ac - 2(a+b+c)d, \tag{30}$$

and $m^{(3)} = 3(a^3 - 3abc + b^3 + c^3 - (a+b+c)d^2)$. Once again, the condition $a \neq b = c$ is required for exact TBM. In this case the neutrino mass eigenvalues become $m_1 = m_0/(a-c+d)$, $m_2 = m_0/(a+2c)$, $m_3 = m_0/(-a+c+d)$, and there is more freedom in choosing parameters, as shown in the scatter plots of $a-c-d$ parameter space in Fig. 8. As in the nonseesaw model, for three singlets hardly any tuning is necessary.

### D. Deviations from TBM in the A-F seesaw model

The seesaw model can be analyzed for deviations from TBM due to VEV misalignment, following the procedure outlined in Sec. II D above, with the same limits for the parameters. The VEV alignment is perturbed as in Eq. (12) and, for the cases of two or three singlets, as in Eq. (13).

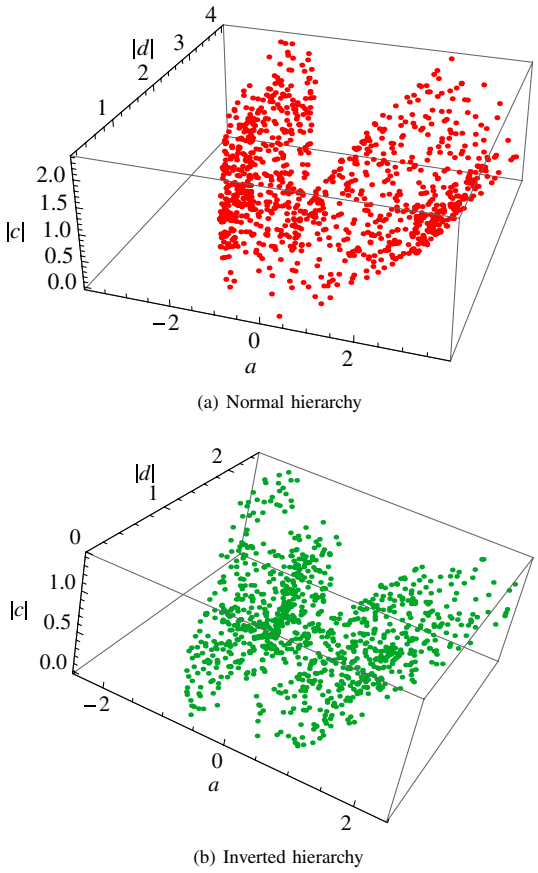


FIG. 8 (color online). Scatter plots of the $a-c-d$ parameter space for the A-F seesaw model, with three Higgs singlet, for normal and inverted hierarchy, with the condition $b = c$.

With the deviated Higgs triplet alignments of Eq. (12), the charged lepton mass matrix is again defined by Eq. (14), and the light neutrino mass matrix is

$$M_\nu^{(1)\prime} = \frac{3m_0}{m^{(1)\prime}} \begin{pmatrix} ((d_1-3a)^2 - 4d_2d_3) & -2d_3^2 + 3ad_2 - d_1d_2 & -2d_2^2 + 3ad_3 - d_1d_3 \\ \cdot & (d_2^2 - 6ad_3 - 4d_1d_3) & 9a^2 + 3d_1a - 2d_1^2 - d_2d_3 \\ \cdot & \cdot & (d_3^2 - 6ad_2 - 4d_1d_2) \end{pmatrix}, \tag{31}$$

$$m^{(1)\prime} = 27a^3 - 9a(d_1^2 + 2d_2d_3) + 2(d_1^3 - 3d_1d_2d_3 + d_2^3 + d_3^3),$$

with $d_1 = d$, $d_2 = d(1+\epsilon_1)$ and $d_3 = d(1+\epsilon_2)$. The deviated neutrino mass matrix for two Higgs singlets is

$$M_\nu^{(2)\prime} = \frac{3m_0}{m^{(2)\prime}} M^{(2)\prime}, \tag{32}$$

where the elements of the symmetric matrix $M^{(2)\prime}$ are

$$M_{11}^{(2)\prime} = d_1^2 - (3c + 2d_2)(3b + 2d_3), \tag{33}$$

$$M_{12}^{(2)\prime} = 9b^2 + 3d_3b - 2d_3^2 + 3cd_1 - d_1d_2, \tag{34}$$

$$M_{13}^{(2)\prime} = 9c^2 + 3d_2c - 2d_2^2 + 3bd_1 - d_1d_3, \tag{35}$$

$$M_{22}^{(2)\prime} = (d_2 - 3c)^2 - 2d_1(3b + 2d_3), \tag{36}$$

$$M_{23}^{(2)\prime} = -2d_1^2 - (d_2 - 3c)(d_3 - 3b), \tag{37}$$

$$M_{33}^{(2)\prime} = (d_3 - 3b)^2 - 2d_1(3c + 2d_2), \tag{38}$$

and

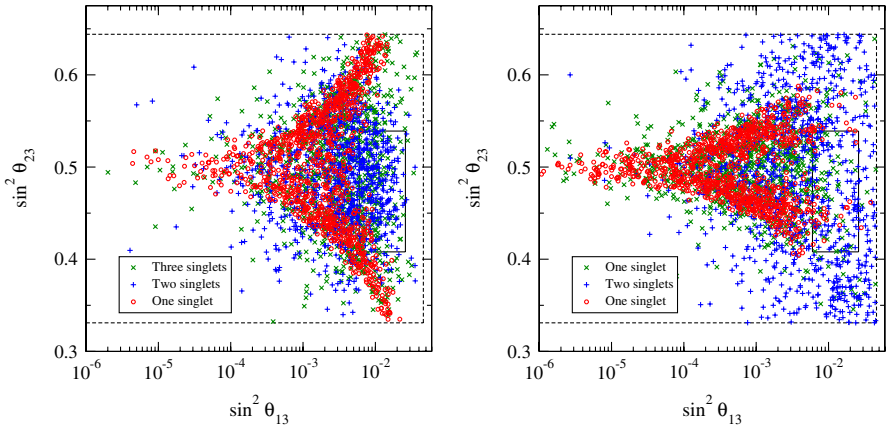


(a) Normal hierarchy (b) Inverted hierarchy

FIG. 9 (color online). Scatter plots of mixing angle observables for the A-F seesaw model [11], with one, two and three Higgs singlets, for both the normal and inverted hierarchy.

$$m^{(2)\prime} = -6d_1(d_2(3b + d_3) + 3cd_3) + (d_3 - 3b)^2(3b + 2d_3) + (d_2 - 3c)^2(3c + 2d_2) + 2d_1^3; \quad (39)$$

for three Higgs singlets, the deviated mass matrix is

$$M'_\nu = \frac{3m_0}{m^{(3)\prime}} M^{(3)\prime}, \quad (40)$$

where the elements of $M^{(3)\prime}$ are

$$M^{(3)\prime}_{11} = (d_1 - 3a)^2 - (3c + 2d_2)(3b + 2d_3), \quad (41)$$

$$M^{(3)\prime}_{12} = 9b^2 + 3d_3b - 2d_3^2 + (d_1 - 3a)(3c - d_2), \quad (42)$$

$$M^{(3)\prime}_{13} = 9c^2 + 3d_2c - 2d_2^2 + 3bd_1 - d_1d_3 + 3a(d_3 - 3b), \quad (43)$$

$$M^{(3)\prime}_{22} = -(3a + 2d_1)(3b + 2d_3) + (d_2 - 3c)^2, \quad (44)$$

$$M^{(3)\prime}_{23} = 9a^2 + 3d_1a - 2d_1^2 + 3b(d_2 - 3c) + 3cd_3 - d_2d_3, \quad (45)$$

$$M^{(3)\prime}_{33} = -(3a + 2d_1)(3c + 2d_2) + (d_3 - 3b)^2, \quad (46)$$

and

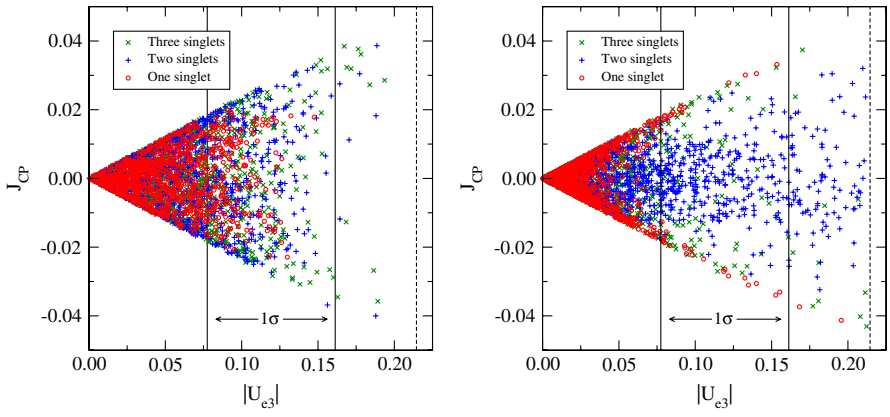


(a) Normal hierarchy (b) Inverted hierarchy

FIG. 10 (color online). Scatter plots of $J_{CP}$ against $|U_{e3}|$ for the A-F seesaw model, with one, two and three Higgs singlets, for both the normal and inverted hierarchy.

$$m^{(3)\prime} = 27a^3 - 9a(9bc + d_1^2 + 2d_2d_3) + 27b^3 - 9b(2d_1d_2 + d_3^2) - 6d_1d_3(3c + d_2) + (d_2 - 3c)^2(3c + 2d_2) + 2d_1^3 + 2d_3^3, \quad (47)$$

with $d_1$, $d_2$ and $d_3$ as defined above. The effect of changing the relative singlet alignment is studied by setting $b = c(1 + \epsilon_3)$ in both the two and three singlet cases.

Figures 9 and 10 show scatter plots for the mixing angles, from diagonalization of Eqs. (31), (32), and (40). Again, there are small differences, and in general the deviations from TBM can become larger with increasing number of singlets. However, there is little discriminative power with regards to the number of singlets, and also with respect to the model treated in Sec. II.

In spite of this, the mass-dependent observables, plotted in Fig. 11, allow some conclusions to be drawn. For instance, in the one singlet case there is a distinct separation of normal and inverted hierarchy, and the normal hierarchy case is very different to the nonseesaw model (Fig. 5). As another example, if the normal mass hierarchy is favored by experiment and $\langle m_{ee} \rangle$ is measured to be 0.05 eV, the upper left panel of Fig. 11 shows that the seesaw model with one singlet can be ruled out. In general, note that deviations from TBM have less effect on the mass observables in the seesaw model.

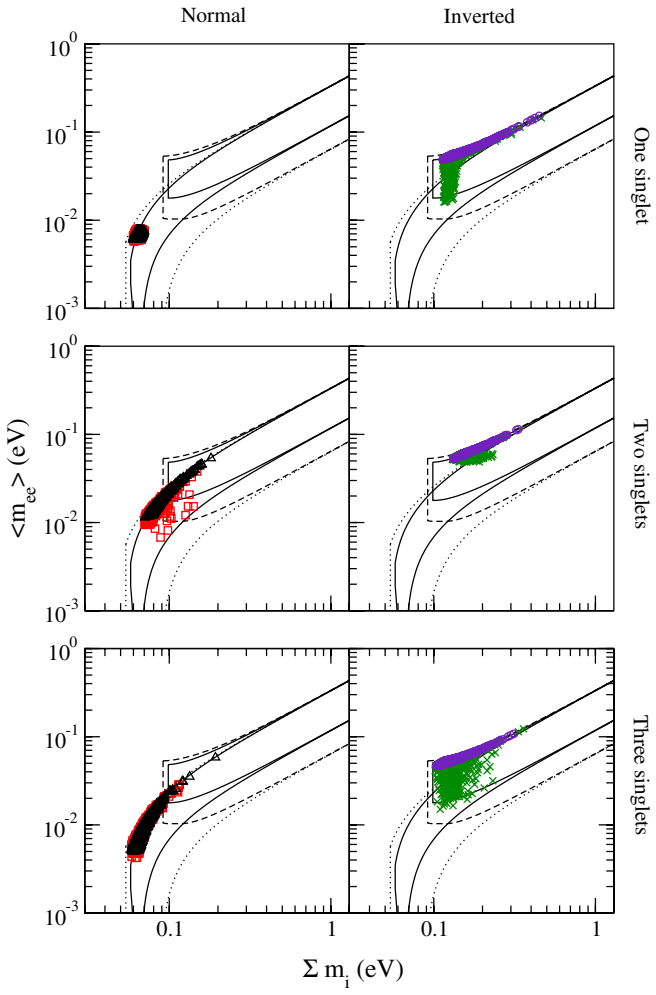


FIG. 11 (color online). Scatter plots of $\langle m_{ee} \rangle$ against $\sum m_i$ for the A-F seesaw model, with one, two and three Higgs singlets, for normal and inverted hierarchy. See the caption of Fig. 5 for an explanation of the symbols used.

## IV. CONCLUSION

The present paper is a study of deviations from TBM due to VEV misalignment in $A_4$ models. After an attempt to classify the vast amount of literature according to the representations of $A_4$ under which the lepton doublets, lepton singlets and seesaw particles transform, two particularly popular examples from classes A and B have been focused on. The models have been checked for tuning and then generalized, in the sense that extra singlets, transforming under representations of $A_4$ that are not used in the original models, are added. In general, the more singlets that are introduced, the less tuning there is. The most general VEV misalignment is allowed for, and the consequences for the lepton mixing observables are studied. Since these quantities have little discriminative power, the focus is shifted to the observables related to neutrino mass. The scatter plots of $\langle m_{ee} \rangle - \sum m_i$ parameter space are different in each model, and allow one to distinguish different models, even after deviation of the VEV alignment. This is an indication of the importance of neutrinoless double beta decay and cosmological mass determination in disentangling neutrino mass models.

## ACKNOWLEDGMENTS

We thank the German Academic Exchange Service (DAAD) for a research grant. This work was supported by the ERC under the Starting Grant MANITOP and by the Deutsche Forschungsgemeinschaft in the Transregio 27 "Neutrinos and beyond—weakly interacting particles in physics, astrophysics and cosmology". J. B. would like to thank Steven Karataglidis for useful discussions and advice throughout the course of this project.

## APPENDIX: $A_4$ TETRAHEDRAL SYMMETRY

The following is an outline of the $A_4$ symmetry group [9,27,74], upon which the models in this analysis are based.

### 1. Introduction to $A_4$

$A_4$ is the alternating group of order 4, and is also the group of all even permutations of four objects, isomorphic to the group of rotational symmetries of the regular tetrahedron. It is a finite, non-Abelian subgroup of SO(3) [35] and SU(3). $A_4$ has 12 elements, which can be divided into 4 conjugacy classes with membership 1, 3, 4 and 4. The dimensionality theorem implies that there are 4 irreducible

TABLE IV. Character table of $A_4$, where $n$ represents the number of elements in each conjugacy class.

| Class | $n$ | $\chi^{1}$ | $\chi^{1'}$ | $\chi^{1''}$ | $\chi^{3}$ |
|---|---|---|---|---|---|
| $C_1$ | 1 | 1 | 1 | 1 | 3 |
| $C_2$ | 4 | 1 | $\omega$ | $\omega^2$ | 0 |
| $C_3$ | 4 | 1 | $\omega^2$ | $\omega$ | 0 |
| $C_4$ | 3 | 1 | 1 | 1 | $-1$ |

representations with dimension $d_j$ such that $\sum_j d_j^2 = 12$. The only solution is $d_1 = d_2 = d_3 = 1$ and $d_4 = 3$, and the representations are labeled as $\underline{1}$, $\underline{1}'$, $\underline{1}''$ and $\underline{3}$, which means that there are three one-dimensional representations and one three-dimensional representation. The character table of $A_4$ is shown in Table IV, with $\omega \equiv e^{i2\pi/3}$ the cube root of unity.[9]

### 2. Different bases for $A_4$

There are two bases for $A_4$ commonly used in lepton family symmetry models: the Ma-Rajasekaran (M-R) basis and the Altarelli-Feruglio (A-F) basis.

#### *a. Ma-Rajasekaran basis*

$A_4$ can be generated by two basic permutations $S$ and $T$, given by $S = (4321)$ and $T = (2314)$, where the generic permutation $(1, 2, 3, 4) \to (n_1, n_2, n_3, n_4)$ is denoted by $(n_1 n_2 n_3 n_4)$. It follows that

$$S^2 = T^3 = (ST)^3 = 1, \tag{A1}$$

which defines a "presentation" of the group. The one-dimensional unitary representations are generated by

$$\begin{aligned} &\underline{1}\text{: } S = 1 \quad T = 1, \\ &\underline{1}'\text{: } S = 1 \quad T = e^{i2\pi/3} \equiv \omega, \\ &\underline{1}''\text{: } S = 1 \quad T = e^{i4\pi/3} \equiv \omega^2, \end{aligned} \tag{A2}$$

and the three-dimensional unitary representation (in this basis) is built up from the generators

$$S = \begin{pmatrix} 1 & 0 & 0 \\ 0 & -1 & 0 \\ 0 & 0 & -1 \end{pmatrix}, \qquad T = \begin{pmatrix} 0 & 1 & 0 \\ 0 & 0 & 1 \\ 1 & 0 & 0 \end{pmatrix}. \tag{A3}$$

The $3 \times 3$ matrices of the natural three-dimensional representation $\underline{3}$ are

$$\begin{aligned} C_1&: \begin{pmatrix} 1 & 0 & 0 \\ 0 & 1 & 0 \\ 0 & 0 & 1 \end{pmatrix}, \\ C_2&: \begin{pmatrix} 0 & 0 & 1 \\ 1 & 0 & 0 \\ 0 & 1 & 0 \end{pmatrix}, \begin{pmatrix} 0 & 0 & 1 \\ -1 & 0 & 0 \\ 0 & -1 & 0 \end{pmatrix}, \begin{pmatrix} 0 & 0 & -1 \\ 1 & 0 & 0 \\ 0 & -1 & 0 \end{pmatrix}, \begin{pmatrix} 0 & 0 & -1 \\ -1 & 0 & 0 \\ 0 & 1 & 0 \end{pmatrix}, \\ C_3&: \begin{pmatrix} 0 & 1 & 0 \\ 0 & 0 & 1 \\ 1 & 0 & 0 \end{pmatrix}, \begin{pmatrix} 0 & 1 & 0 \\ 0 & 0 & -1 \\ -1 & 0 & 0 \end{pmatrix}, \begin{pmatrix} 0 & -1 & 0 \\ 0 & 0 & 1 \\ -1 & 0 & 0 \end{pmatrix}, \begin{pmatrix} 0 & -1 & 0 \\ 0 & 0 & -1 \\ 1 & 0 & 0 \end{pmatrix}, \\ C_4&: \begin{pmatrix} 1 & 0 & 0 \\ 0 & -1 & 0 \\ 0 & 0 & -1 \end{pmatrix}, \begin{pmatrix} -1 & 0 & 0 \\ 0 & 1 & 0 \\ 0 & 0 & -1 \end{pmatrix}, \begin{pmatrix} -1 & 0 & 0 \\ 0 & -1 & 0 \\ 0 & 0 & 1 \end{pmatrix}, \end{aligned} \tag{A4}$$

where each matrix can be generated by $S$ and $T$ in Eq. (A3). It is evident that the characters of the $\underline{3}$ representation (the last column of Table IV) are simply the traces of the matrices in each class.

The multiplication rules are given by

$$\underline{1} \times \underline{1} = \underline{1}, \tag{A5}$$

$$\underline{1}' \times \underline{1}'' = \underline{1}, \tag{A6}$$

$$\underline{1}'' \times \underline{1}' = \underline{1}, \tag{A7}$$

$$\underline{1}' \times \underline{1}' = \underline{1}'', \tag{A8}$$

$$\underline{1}'' \times \underline{1}'' = \underline{1}', \tag{A9}$$

$$\underline{3} \times \underline{3} = \underline{1} + \underline{1}' + 1'' + \underline{3}_{as} + \underline{3}_{s}, \tag{A10}$$

where $\underline{3}_{as}$ and $\underline{3}_{s}$ are "asymmetric" and "symmetric" combinations, respectively. If $\underline{3}_a \sim (a_1, a_2, a_3)$ and $\underline{3}_b \sim (b_1, b_2, b_3)$ are two triplets transforming by the matrices in Eq. (A4), then the three singlets and two triplets in the product in Eq. (A10) are

[9]Note that $\omega = e^{i2\pi/3} = -1/2 + \sqrt{3}/2$ satisfies $\omega^2 = \omega^*$ and $1 + \omega + \omega^2 = 0$.

$$\underline{1} = a_1 b_1 + a_2 b_2 + a_3 b_3, \tag{A11}$$

$$\underline{1}' = a_1 b_1 + \omega^2 a_2 b_2 + \omega a_3 b_3, \tag{A12}$$

$$\underline{1}'' = a_1 b_1 + \omega a_2 b_2 + \omega^2 a_3 b_3, \tag{A13}$$

$$\underline{3}_1 \sim (a_2 b_3, a_3 b_1, a_1 b_2), \tag{A14}$$

$$\underline{3}_2 \sim (a_3 b_2, a_1 b_3, a_2 b_1). \tag{A15}$$

#### b. Altarelli-Feruglio basis

In the M-R basis, the generator $S$ in Eq. (A3) is diagonal. However, one can also represent $A_4$ in a basis where $T$ is diagonal, obtained through the unitary transformation:

$$T' = V^\dagger T V = \begin{pmatrix} 1 & 0 & 0 \\ 0 & \omega & 0 \\ 0 & 0 & \omega^2 \end{pmatrix}, \tag{A16}$$

$$S' = V^\dagger S V = \frac{1}{3}\begin{pmatrix} -1 & 2 & 2 \\ 2 & -1 & 2 \\ 2 & 2 & -1 \end{pmatrix}, \tag{A17}$$

where

$$V = \frac{1}{\sqrt{3}}\begin{pmatrix} 1 & 1 & 1 \\ 1 & \omega^2 & \omega \\ 1 & \omega & \omega^2 \end{pmatrix}. \tag{A18}$$

It is known that the most general mass matrix leading to TBM,

$$m_\nu^{\mathrm{TBM}} = \begin{pmatrix} A & B & B \\ \cdot & \frac{1}{2}(A+B+D) & \frac{1}{2}(A+B-D) \\ \cdot & \cdot & \frac{1}{2}(A+B+D) \end{pmatrix} \tag{A19}$$

is invariant with respect to $S'$ : $(S')^T m_\nu^{\mathrm{TBM}} S' = m_\nu^{\mathrm{TBM}}$. Note that the matrix $V$ is the so-called "magic matrix,", which appears in some $A_4$ models as the unitary matrix that diagonalizes the charged lepton mass matrix. In the $S'$, $T'$ basis, the multiplication rules are identical to those in Eqs. (A5)–(A10), but the product of two triplets gives the composition of the following irreducible representations:

$$\underline{1} = a_1 b_1 + a_2 b_3 + a_3 b_2, \tag{A20}$$

$$\underline{1}' = a_3 b_3 + a_1 b_2 + a_2 b_1, \tag{A21}$$

$$\underline{1}'' = a_2 b_2 + a_1 b_3 + a_3 b_1, \tag{A22}$$

$$\underline{3}_s \sim \frac{1}{3}(2a_1 b_1 - a_2 b_3 - a_3 b_2, 2a_3 b_3 - a_1 b_2 - a_2 b_1, 2a_2 b_2 - a_1 b_3 - a_3 b_1), \tag{A23}$$

$$\underline{3}_{as} \sim \frac{1}{3}(a_2 b_3 - a_3 b_2, a_1 b_2 - a_2 b_1, a_1 b_3 - a_3 b_1). \tag{A24}$$

### 3. Equivalence of the two bases

The model presented in Sec. II A can be formulated in the M-R basis, using the same particle assignments and the Lagrangian in Eq. (3). With the product decomposition rules in Eqs. (A11)–(A15), and the triplet VEV alignment

$$\langle \varphi \rangle = (v, v, v) \quad \text{and} \quad \langle \varphi' \rangle = (v', 0, 0), \tag{A25}$$

the charged lepton and neutrino mass matrices are

$$M_\ell = v_d \frac{v}{\Lambda}\begin{pmatrix} y_e & y_e & y_e \\ y_\mu & y_\mu \omega^2 & y_\mu \omega \\ y_\tau & y_\tau \omega & y_\tau \omega^2 \end{pmatrix}, \qquad M_\nu = \frac{v_u}{\Lambda}\begin{pmatrix} a & 0 & 0 \\ \cdot & a & d \\ \cdot & \cdot & a \end{pmatrix}. \tag{A26}$$

In this case, $M_\ell$ is diagonalized by the magic matrix [Eq. (A18)], and $M_\nu$ is diagonalized by

$$V_\nu = \begin{pmatrix} 0 & 1 & 0 \\ \frac{1}{\sqrt{2}} & 0 & -\frac{1}{\sqrt{2}} \\ \frac{1}{\sqrt{2}} & 0 & \frac{1}{\sqrt{2}} \end{pmatrix}, \tag{A27}$$

which combines with $V$ in Eq. (A18) to give $U_{\mathrm{TBM}}$. The neutrino mass matrix in Eq. (A26) is equivalent to that in Eq. (7), with the change of basis induced by $V$. Thus the two bases lead to equivalent models, with the triplet VEV alignments in the charged lepton and neutrino sectors effectively swapped [compare Eqs. (4) and (A25)]. Note that the change of basis will change the relative phases of the eigenvalues of $M_\nu$.


[1] G. L. Fogli, E. Lisi, A. Marrone, and A. Palazzo, Prog. Part. Nucl. Phys. **57**, 742 (2006).
[2] G. L. Fogli *et al.*, Phys. Rev. D **75**, 053001 (2007).
[3] G. L. Fogli *et al.*, Phys. Rev. D **78**, 033010 (2008).
[4] T. Schwetz, M. Tortola, and J. W. F. Valle, New J. Phys. **10**, 113011 (2008).
[5] P. F. Harrison, D. H. Perkins, and W. G. Scott, Phys. Lett. B **530**, 167 (2002).
[6] S. Pakvasa, W. Rodejohann, and T. J. Weiler, Phys. Rev. Lett. **100**, 111801 (2008).
[7] G. Altarelli and F. Feruglio, arXiv:1002.0211.
[8] G. Altarelli and F. Feruglio, Nucl. Phys. **B720**, 64 (2005).

[9] A. Zee, Phys. Lett. B **630**, 58 (2005).
[10] B. Adhikary, B. Brahmachari, A. Ghosal, E. Ma, and M. K. Parida, Phys. Lett. B **638**, 345 (2006).
[11] G. Altarelli and F. Feruglio, Nucl. Phys. **B741**, 215 (2006).
[12] M. Honda and M. Tanimoto, Prog. Theor. Phys. **119**, 583 (2008).
[13] B. Brahmachari, S. Choubey, and M. Mitra, Phys. Rev. D **77**, 073008 (2008).
[14] F. Feruglio, C. Hagedorn, Y. Lin, and L. Merlo, Nucl. Phys. **B809**, 218 (2009).
[15] S. Morisi, Phys. Rev. D **79**, 033008 (2009).
[16] S. Morisi, J. Phys. Conf. Ser. **203**, 012060 (2010).
[17] G. Altarelli, F. Feruglio, and Y. Lin, Nucl. Phys. **B775**, 31 (2007).
[18] F. Bazzocchi, S. Kaneko, and S. Morisi, J. High Energy Phys. 03 (2008) 063.
[19] E. Ma, Phys. Rev. D **70**, 031901 (2004).
[20] E. Ma, Phys. Rev. D **72**, 037301 (2005).
[21] E. Ma, Mod. Phys. Lett. A **17**, 627 (2002).
[22] K. S. Babu, E. Ma, and J. W. F. Valle, Phys. Lett. B **552**, 207 (2003).
[23] M. Hirsch, J. C. Romao, S. Skadhauge, J. W. F. Valle, and A. Villanova del Moral, Phys. Rev. D **69**, 093006 (2004).
[24] X.-G. He, Y.-Y. Keum, and R. R. Volkas, J. High Energy Phys. 04 (2006) 039.
[25] G. Altarelli, F. Feruglio, and C. Hagedorn, J. High Energy Phys. 03 (2008) 052.
[26] T. J. Burrows and S. F. King, arXiv:0909.1433.
[27] E. Ma and G. Rajasekaran, Phys. Rev. D **64**, 113012 (2001).
[28] K. S. Babu and X.-G. He, arXiv:hep-ph/0507217.
[29] E. Ma, Phys. Rev. D **73**, 057304 (2006).
[30] F. Yin, Phys. Rev. D **75**, 073010 (2007).
[31] B. Adhikary and A. Ghosal, Phys. Rev. D **78**, 073007 (2008).
[32] C. Csaki, C. Delaunay, C. Grojean, and Y. Grossman, J. High Energy Phys. 10 (2008) 055.
[33] M.-C. Chen and S. F. King, J. High Energy Phys. 06 (2009) 072.
[34] A. Hayakawa, H. Ishimori, Y. Shimizu, and M. Tanimoto, Phys. Lett. B **680**, 334 (2009).
[35] J. Berger and Y. Grossman, J. High Energy Phys. 02 (2010) 071.
[36] G.-J. Ding and J.-F. Liu, arXiv:0911.4799.
[37] M. Mitra, arXiv:0912.5291.
[38] F. del Aguila, A. Carmona, and J. Santiago, arXiv:1001.5151.
[39] P. V. Dong, L. T. Hue, H. N. Long, and D. V. Soa, Phys. Rev. D **81**, 053004 (2010).
[40] E. Ma, Mod. Phys. Lett. A **22**, 101 (2007).
[41] E. Ma, Mod. Phys. Lett. A **21**, 2931 (2006).
[42] F. Bazzocchi, S. Morisi, and M. Picariello, Phys. Lett. B **659**, 628 (2008).
[43] E. Ma, arXiv:0908.3165.
[44] M. Hirsch, A. Villanova del Moral, J. W. F. Valle, and E. Ma, Phys. Rev. D **72**, 091301 (2005).
[45] S. Morisi, M. Picariello, and E. Torrente-Lujan, Phys. Rev. D **75**, 075015 (2007).
[46] P. Ciafaloni, M. Picariello, E. Torrente-Lujan, and A. Urbano, Phys. Rev. D **79**, 116010 (2009).
[47] M. Hirsch, S. Morisi, and J. W. F. Valle, Phys. Rev. D **78**, 093007 (2008).
[48] S. Morisi and E. Peinado, Phys. Rev. D **80**, 113011 (2009).
[49] S.-L. Chen, M. Frigerio, and E. Ma, Nucl. Phys. **B724**, 423 (2005).
[50] F. Bazzocchi, M. Frigerio, and S. Morisi, Phys. Rev. D **78**, 116018 (2008).
[51] F. Bazzocchi, S. Morisi, M. Picariello, and E. Torrente-Lujan, J. Phys. G **36**, 015002 (2009).
[52] P. Ciafaloni, M. Picariello, A. Urbano, and E. Torrente-Lujan, Phys. Rev. D **81**, 016004 (2010).
[53] E. Ma, Mod. Phys. Lett. A **20**, 2601 (2005).
[54] L. Lavoura and H. Kuhbock, Mod. Phys. Lett. A **22**, 181 (2007).
[55] M. Hirsch, A. S. Joshipura, S. Kaneko, and J. W. F. Valle, Phys. Rev. Lett. **99**, 151802 (2007).
[56] P. H. Frampton and S. Matsuzaki, arXiv:0806.4592.
[57] Y. Lin, Nucl. Phys. **B813**, 91 (2009).
[58] S. F. King and M. Malinsky, Phys. Lett. B **645**, 351 (2007).
[59] G. Altarelli and D. Meloni, J. Phys. G **36**, 085005 (2009).
[60] Y. Lin, Nucl. Phys. **B824**, 95 (2010).
[61] S. Morisi, Nuovo Cimento B **123**, 886 (2008).
[62] M. Hirsch, S. Morisi, and J. W. F. Valle, Phys. Lett. B **679**, 454 (2009).
[63] D. Ibanez, S. Morisi, and J. W. F. Valle, Phys. Rev. D **80**, 053015 (2009).
[64] G.-J. Ding, Nucl. Phys. **B827**, 82 (2010).
[65] F. Bazzocchi, L. Merlo, and S. Morisi, Nucl. Phys. **B816**, 204 (2009).
[66] F. Plentinger and W. Rodejohann, Phys. Lett. B **625**, 264 (2005).
[67] A. Dighe, S. Goswami, and W. Rodejohann, Phys. Rev. D **75**, 073023 (2007).
[68] M. Hirsch, E. Ma, J. C. Romao, J. W. F. Valle, and A. Villanova del Moral, Phys. Rev. D **75**, 053006 (2007).
[69] K. A. Hochmuth, S. T. Petcov, and W. Rodejohann, Phys. Lett. B **654**, 177 (2007).
[70] C. H. Albright and W. Rodejohann, Phys. Lett. B **665**, 378 (2008).
[71] S. Goswami, S. T. Petcov, S. Ray, and W. Rodejohann, Phys. Rev. D **80**, 053013 (2009).
[72] Y. F. Li and Q. Y. Liu, Mod. Phys. Lett. A **25**, 63 (2010).
[73] S.-F. Ge, H.-J. He, and F.-R. Yin, arXiv:1001.0940.
[74] G. Altarelli, arXiv:0711.0161.